V.V. TETYORKIN,[1] A.I. TKACHUK,[2] I.G. LUTSYSHYN[1]

[1] V.E. Lashkaryov Institute of Semiconductor Physics, Nat. Acad. of Sci. of Ukraine
(41, Nauky Ave., Kyiv, 03028, Ukraine; e-mail: teterkin@meta.ua)
[2] Volodymyr Vynnychenko Central Ukrainian State University
(1, Shevchenka Str., Kropyvnytskyi 25006, Ukraine; e-mail: atkachuk08@meta.ua)

UDC 539

RECOMBINATION AND TRAPPING OF EXCESS CARRIERS IN *n*-InSb

The effect of trapping on the transient and steady-state lifetimes of excess carriers is investigated in InSb of n-type conductivity. Photoconductive decay and direct current measurements are used to characterize the starting material and infrared photodiodes. The large difference between the transient and steady-state lifetimes is explained by the trapping of minority carriers at the acceptor centers within the two-level recombination model. The recombination parameters of the traps are estimated.

K e y w o r d s: InSb, lifetime, recombination and trapping effects, infrared photodiodes.

1. Introduction

The lifetime of excess carriers is an important parameter characterizing narrow-gap semiconductors themselves and infrared photodiodes based on them. A thorough analysis of the experimental methods that can be used to measure steady-state and transient lifetimes in these materials was performed by Lopes *et al.* [11]. In this work, the transient lifetime of majority carriers and the steady-state lifetime of minority carriers were determined on the basis of photoconductive decay (PCD) measurements in materials and current-voltage characteristics in photodiodes. Both methods are known to give equivalent results, when the minority carrier trapping can be neglected. A significant difference between steady-state and transient lifetimes indicates the presence of trapping effects.

C i t a t i o n: Tetyorkin V.V., Tkachuk A.I., Lutsyshyn I.G. Recombination and trapping of excess carriers in *n*-InSb. *Ukr. J. Phys.* **69**, No. 1, 45 (2024). https://doi.org/10.15407/ujpe69.1.45.

Ц и т у в а н н я: Тетьоркін В.В., Ткачук А.І., Луцишин І.Г. Рекомбінація та прилипання нерівноважних носіїв в *n*-InSb. *Укр. фіз. журн.* **69**, № 1, 45 (2024).

The main recombination mechanisms in n-InSb are radiative, Auger-1 and Shockley–Reed–Hall (SRH) ones [2]. It is the latter that dominates at the operating temperatures of InSb-based photodiodes. Theoretical models of SRH recombination were developed in early works [3, 4]. It was shown that the lifetime of excess carriers is determined by two donor-like centers with energy levels located above the edge of the valence band at distances close to $E_g/4$ and $E_g/2$ (hereinafter referred to as levels $E1$ and $E2$, respectively). Within the framework of these models, the capture of minority carriers in a p-type material was explained. It has also been suggested that the same centers may be responsible for the recombination of excess carriers in the n-type material. However, a detailed analysis of this suggestion has not been carried out. Subsequently, the acceptor- and donor-type traps were discovered in the n-type material by the DLTS method, the recombination parameters of which differed significantly from those used in [5, 6]. The minority carrier trapping has been observed in infrared photodiodes fabricated on the n-type material [7]. Because traps in infrared photodiodes can be responsible for the tunneling current and

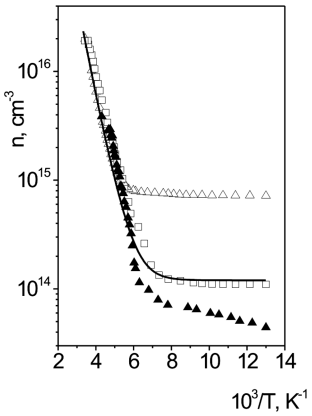

Fig. 1. Temperature dependences of the electron density in reference and heat-treated samples (open and closed dots, respectively). The solid curve is the theoretical fit (see text)

low-frequency noise that degrades their performance [8, 9], their identification remains an important issue. To the best of the authors' knowledge, the minority carrier trapping in n-InSb and photodiodes based on it has not yet been discussed in the literature.

In this work, the effect of recombination-active traps, which can interact with both energy bands, on the lifetime of excess carriers is examined. The difference between recombination centers and traps is that the latter are characterized by a significant asymmetry in the capture coefficients of minority and majority carriers. Based on experimental data, the density of trapping centers and their energy position were estimated.

2. Experimental

Wafers of n-InSb(100) grown by the Czochralski method were used for the investigation. The dislocation density was less than 10^3 cm^{-2}. The density and mobility of electrons determined from the Hall-effect measurements were in the intervals 10^{14}–3×10^{15} cm^{-3} and 2–3×10^5 cm^2/V s respectively, at 77 K. Reference samples ∼500 μm thick were subjected to the chemical-mechanical polishing in an HBr + 2.0% Br_2 solution to a thickness of about 350 μm. The final treatment included their immersion in the CP4A etchant for several minutes and passivation of both surfaces in an alcoholic solution of sodium sulfide. Before photoelectrical measurements, the samples were stored in isopropanol to prevent the effect of atmospheric moisture on the surface. Photodiodes were fabricated by the Cd diffusion at temperatures near 400 °C. Fabrication details have been described earlier [10]. Direct current (DC) and high-frequency (1 MHz) capacitance measurements were used to characterize the photodiodes.

A C8-13 storage oscilloscope with a frequency band of 0.8 GHz was used to measure the photoconductive decay. The excitation of the excess carriers was carried out by a Q-switched Nd : YAG laser with a pulse duration of ∼20 ns and the pulse raise and fall time close to 5 ns. The intensity of laser radiation was attenuated using neutral filters and measured using a calibrated pyroelectric photodetector. PCD was measured according to the standard method and recorded as a decrease in the voltage across the series resistance, $\Delta\sigma/\sigma_0 = \Delta U/U_0$. The photon flux falling on the surface of the sample was of the order of 1×10^{16} cm^{2}s^{-1}, which corresponded to the mode of low injection level. In order to prevent the sweep out effect for minority carriers, the dark current varied within 1–5 mA. It was established that the magnitude of the measured signal increases linearly with the current, which indicates its absence. The decay waveforms were memorized, digitized, and stored for the theoretical analysis. Hall-effect measurements in a field of 2 kOe were carried out in the temperature region of 77–300 K to determine the density and mobility of equilibrium carriers. PCD and Hall-effect measurements were performed before and after the fabrication of the $p - n$ junctions to study the effect of the thermal treatment to which the samples are subjected during the processing on their electrical and photovoltaic properties. The depth of the diffusion layer was determined by probe measurements of a thermoEMF during its precision chemical etching. The thickness of the samples after the etching was about 300 μm. Below, these samples are referred to as heat-treated.

3. Results and Discussion

Typical temperature dependences of the electron density in reference and heat-treated samples are presented in Fig. 1. In heat-treated samples, the Hall effect measurements were made by Van der Pauw method. These samples retained the n-type conductivity, but the electron mobility decreased by 3–5 times. In a number of samples, the freezing of electrons was observed as shown in Fig. 1. It can be concluded that, as a result of the heat treatment of the starting material during the fabrication of photodi-

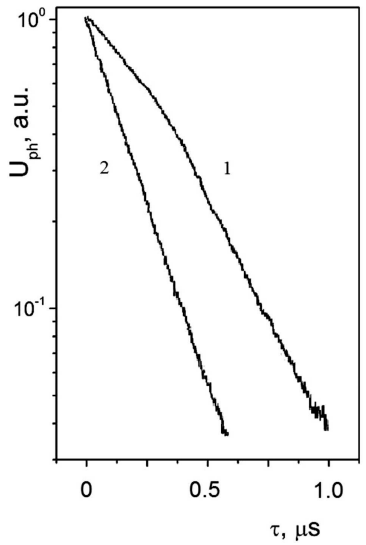

Fig. 2. Normalized PCD waveforms in a heat-treated sample at 77 K (*1*) and 173 K (*2*)

odes, the degree of its compensation increases due to the generation of acceptor-type defects. In the reference samples, the density of equilibrium electrons n_0 as a function of the temperature can be well approximated by the expression

$$n_0(T) = n_{77} + n_i(T), \qquad (1)$$

where n_{77} and $n_i(T)$ are the density of electrons at 77 K and the density of intrinsic carriers, respectively. This approximation satisfactorily describes experimental dependences for the values of $n_0 \leq \leq 3 \times 10^{15}$ cm^{-3} at 77 K.

Namely, the waveforms were composed of slow and fast decays in the temperature region from 77 K to approximately 120 K. At a further increase in the temperature, a single exponent decay was again observed. The carrier lifetimes were determined from the $1/e$ point of the normalized decay waveforms plotted on a linear scale. The results are shown in Figs. 3 and 4 for reference and heat-treated samples.

The normalized waveforms of PCD are shown in Fig. 2. In the reference samples, the waveforms (not shown here) were represented by a single exponent, while, in the heat-treated ones, they exhibited a more complex behavior depending on the carrier density and temperature.

To explain the experimental data in reference samples, a single-level recombination level and an arbitrary density of recombination centers N_t were assumed. Data on heat-treated samples were considered within the framework of a two-level model, including acceptor-type traps. For comparison, Fig. 3 also shows the results of calculating the lifetime

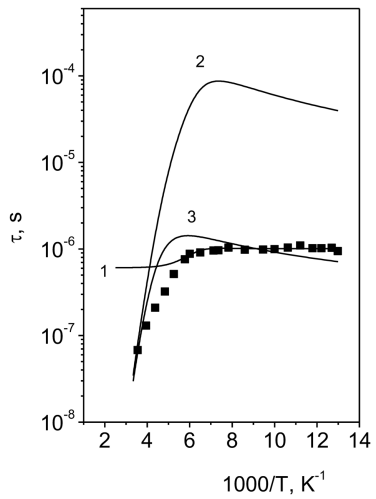

Fig. 3. Experimental (dots) and calculated *1*transient lifetime in a reference sample with an electron density of $1.05 \times \times 10^{14}$ cm^{-3}. Curves *2* and *3* are the Auger-1 lifetime calculated for electron densities of 1×10^{14} cm^{-3} and 1×10^{15} cm^{-3}, respectively

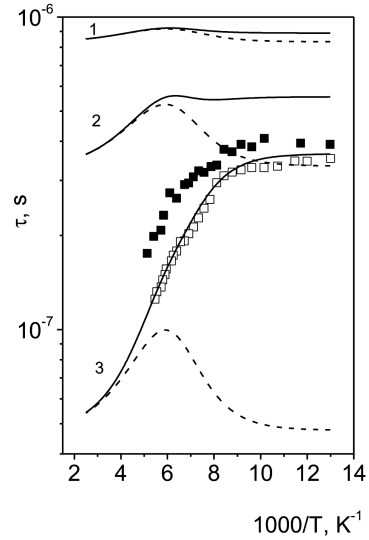

Fig. 4. Experimental lifetimes in heat-treated samples with electron densities of 9.5×10^{13} and 9.0×10^{13} cm^{-3} (closed and open dots, respectively). The solid and dashed curves represent the lifetimes of majority and minority carriers, respectively, calculated for the density of acceptor traps N_{t3} cm^{-3}: 1×10^{11} (*1*), 1×10^{12} (*2*) and 1×10^{13} (*3*)

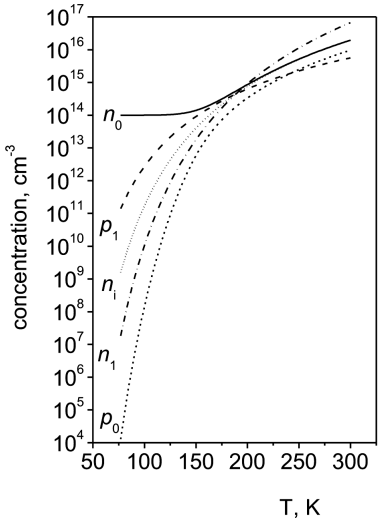

Fig. 5. Temperature dependences of the equilibrium densities of electrons, holes, intrinsic carriers n_i and recombination parameters n_1 and p_1, calculated for the $E2$ level in the middle of the band gap with the density $N_{t2} = 1 \times 10^{14}$ cm^{-3}

for the Auger-1 recombination mechanism (see Appendix). According to Shockley and Read [11], the steady-state lifetime of excess electrons and holes for a low injection and single-level recombination is given by

$$\tau_n = \left(\frac{\tau_{p0}\,(n_0 + n_1) + \tau_{n0}\,[p_0 + p_1 + N_t f_t]}{n_0 + p_0 + N_t f_t\,(1 - f_t)}\right) \tag{2}$$

and

$$\tau_p = \left(\frac{\tau_{n0}\,(p_0 + p_1) + \tau_{p0}\,[n_0 + n_1 + N_t\,(1 - f_t)]}{n_0 + p_0 + N_t f_t\,(1 - f_t)}\right), \tag{3}$$

where $n_1 = n_0 \exp\,[(E_t - E_F)/kT)]$, $p_1 = p_0 \times$ $\times \exp\,[(E_F - E_t)/kT]$, $\tau_{n0} = (N_t C_n)^{-1}$, $\tau_{p0} =$ $= (N_t C_p)^{-1}$, E_t is the recombination level energy, C_n and C_p are the capture coefficients for electrons and holes, $f_t = n_0/(n_0 + n_1) = p_1/(p_0 + p_1)$, $1 - f_t =$ $= n_1/(n_0 + n_1) = p_0/(p_0 + p_1)$, f_t is the probability of the level occupancy with electrons. Since the values of N_t and n_0 in n-InSb can be comparable, the approach of SRH recombination with an arbitrary density of centers is justified.

According to Sandiford [12] and Wertheim [13], the transient lifetime in this model is represented by two time constants

$$\tau_i = \Big\{C_p\,[p_0 + p_1 + N_t f_t] + \\ + C_n\,[n_0 + n_1 + N_t\,(1 - f_t)]\Big\}^{-1} \tag{4}$$

and

$$\tau_t = \frac{\left[\begin{array}{l}(C_n N_t)^{-1}\,[p_0 + p_1 + N_t f_t] + \\ + (C_p N_t)^{-1}\,[n_0 + n_1 + N_t\,(1 - f_t)]\end{array}\right]}{n_0 + p_0 + N_t f_t (1 - f_t)}, \tag{5}$$

where the response time τ_i is associated with the readjustment in the center occupancy related to the abrupt termination of the optical injection, and τ_t is the transient lifetime associated with the recombination time. As can be seen from the above expressions, the steady-state lifetime of minority carriers and the transient lifetime are different. They can be equal only at small values of N_t.

At temperatures close to 77 K, Eqs. (2), (3), and (5) can be simplified in view of the relationships between the density of majority n_0 and minority p_0 carriers and the recombination parameters n_1 and p_1 for the mid-gap level, Fig. 5. In the calculation, the density of recombination centers N_t was assumed to be equal to n_{77}, and the band parameters of InSb were taken from [2]. After simplifications, the following expressions were obtained:

$$\tau_p \approx \tau_{p0} = 1/C_p N_t, \tag{6}$$

$$\tau_n \approx \tau_t \approx 1/C_p N_t + 1/C_n n_0. \tag{7}$$

The physical meaning of Eqs. (6) and (7) is as follows. The recombination process includes two stages: the capture of minority carriers (holes) to centers occupied by electrons with a characteristic time τ_p, and the subsequent fast capture of excess electrons from the conduction band. For a particular case of the $E2$ level, located at the middle of the gap, the capture coefficients are $C_{n2} \approx 10^{-6}$ cm^{3}s^{-1} and $C_{p2} \approx 10^{-8}$ cm^{3}s^{-1} [4]. At $N_{t2} \approx n_0$, the lifetime of holes $\tau_p = (C_{p2} N_{t2})^{-1}$ is of the order of 10^{-6} s. Since the value of $(C_{n2} n_0)^{-1}$ is about 10^{-8} s, this leads to $\tau_p \approx \tau_n$, which is typical of recombination centers. Since the filling of the $E2$ level with electrons varies slightly with the temperature, the transient lifetime remains virtually unchanged up to approximately 200 K. It is obvious that, in n-InSb, there is no trapping of minority carriers, since the recombination occurs with the participation of donor-like centers.

The trapping of minority carriers implies the existence of acceptor-type traps in the n-type material. In this case, the charge neutrality is expressed

as $\delta n = \delta p + \delta p_t$, where δp_t is the density of trapped holes. In this case, the lifetimes of electrons and holes are different, with $\tau_n > \tau_p$, where the lifetime of electrons is determined by relation (7). In a good approximation, the transient constants in Eqs. (4) and (5) are determined by the lifetimes of minority and majority carriers, i.e., $\tau_i \approx \tau_p$ and $\tau_t \approx \tau_n$ [9]. Thus, the significant trapping of minority carriers means that the ratio $R = C_p N_t / C_n n_0$ is greater than one. Obviously, a large ratio of capture cross sections C_p/C_n contributes to the effective hole trapping.

The PCD waveforms shown in Fig. 2 may indicate the capture of minority carriers in heat-treated samples. Two-stage PCD was described in detail by Blackmore and Nomura [14]. It has been shown that the shape of the PCD signal can be different, by depending on the capture of minority or majority carriers at the initial stage of decay. Namely, the capture of minority carriers leads to a slow decay at the first stage, and a fast decay at the second. Since the acceptor traps in the studied samples are initially occupied by electrons, they are unavailable for the participation in the recombination process. Therefore, the hole capture must occur before the electron capture, resulting in two slopes of the decay waveform.

Theoretically, PCD in narrow-gap semiconductors with trapping centers was studied by Reichman [15]. The condition for the excitation pulse width to be shorter than the smallest carrier lifetime was examined. In this case, the charge neutrality $\delta n = \delta p$ is realized at the initial stage of the decay of excess carriers. For a low injection of excess carriers, the PCD signal is linearly proportional to the photoconductivity response

$$\delta\sigma(t) = q\mu_p \left[b\delta n(t) + \delta p(t)\right], \tag{8}$$

where μ_p is the hole mobility, b is the ratio of the electron mobility to the hole one, q is the charge of the electron. Since the electron mobility in InSb by approximately two orders of magnitude exceeds the hole mobility, to a good approximation, the measured signal is determined by the decay of excess electrons. For the n-type material, the following solution was obtained:

$$\delta n(t) = \frac{1}{1-R}\exp\left(-\frac{t}{\tau_{p0}}\right) - \frac{R}{1-R}\exp\left(-\frac{t}{R\tau_{p0}}\right). \tag{9}$$

As can be seen, the PCD waveform depends on the degree of minority carrier trapping $R = C_{p3}N_{t3}/C_{n3}n_0$.

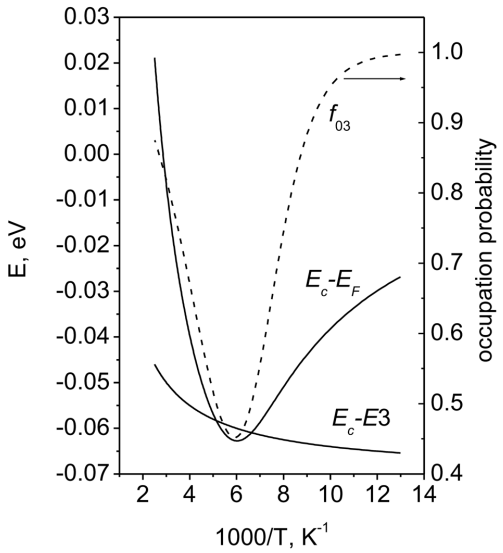

Fig. 6. Energy position of Fermi and $E3$ levels (solid curves) and occupation probability f_{03} (dashed curve) as a function of the temperature

The effect of low, intermediate, and high values of R (0.1, 2, and 10, respectively) was analyzed. When $R = 0.1$, the trapping is negligible, thus making the majority and minority carrier lifetimes approximately equal. The decay of excess carriers is mainly determined by the first term of the above equation with the time constant τ_{p0}. For an intermediate value of $R = 2$, both exponents can contribute to the PCD waveform which contains slow and fast decays. When $R = 10$, the PCD is determined by the second term in (9), and the waveform is again represented by a single exponential, but with the time constant $R\tau_{p0}$. Conditions for the intermediate R, apparently, took place at temperatures close to 77 K in measured samples with an electron density close to 10^{14} cm^{-3}. As the temperature increases, the filling of the $E3$ level by electrons decreases, and traps can act as recombination centers, resulting in a single exponential waveform at temperatures around 160–170 K.

To explain experimental data shown in Fig. 4, *a*, the model was used that includes a donor-like recombination level $E2$ and an acceptor-like trapping level $E3$, Fig. 6. Acceptor-like traps in InSb were reported in a number of works [5, 6, 16, 17]. Assuming that the $E2$ and $E3$ levels do not interact, the total recombination rate can be represented as the sum of the recombination rates of individual levels [13, 18] (see Appendix). At the first stage of recombination,

holes are captured on $E2$ and $E3$ levels occupied by electrons, so the lifetime of minority carriers can be expressed as

$$\frac{1}{\tau_p} = \frac{1}{\tau_{p2}} + \frac{1}{\tau_{p3}} = (C_{p2}N_{t2} + C_{p3}N_{t3}f_{t3})^{-1}, \qquad (10)$$

where $f_{t3} = n_0/(n_0+n_{13})$ is the occupation probability of the $E3$ level by electrons. The subscripts 2 and 3 denote energy levels $E2$ and $E3$, respectively. For the majority carriers, the lifetime is given by

$$\tau_n = \left[1 + \frac{C_{p3}N_{t3}}{C_{n3}n_0} f_{t3}^2\right] \tau_p = \left(1 + R_3 f_{t3}^2\right) \tau_p. \qquad (11)$$

The energy position of the trap level as a function of the temperature was taken to be $E_{t3} = 0.07\text{–}6 \times \times 10^{-5}\, T$ eV, Fig. 6, which is close to the value used in [17]. To fit the experimental date, the density of traps N_{t3} was varied from 1×10^{11} to 1×10^{13} cm^{-3}, Fig. 4. The best agreement was obtained for the capture coefficients $C_{n3} = 3 \times 10^{-8}$ s and $C_{p3} = 2 \times 10^{-6}$ s. As can be seen, at low values of N_t, the trapping effect is negligible. Therefore, the lifetime of the majority and minority carriers is approximately the same and is determined by the $E2$ level. As the density of traps increases, their influence on the lifetime increases and, at $N_{t3} = 10^{13}$ cm^{-3}, it is completely determined by traps. As a result, a pronounced difference arises between the lifetimes of majority and minority carriers.

Note that the PCD waveform composed of two slopes, when are plotted on the logarithmic scale, can also be observed due to the surface recombination. The fact is that PCD measures an effective carrier lifetime $1/\tau_{\text{eff}} = (1/\tau_B) + (1/\tau_S)$, where τ_B and τ_S are the bulk and surface lifetimes, accordingly [19, 20]. If the carrier lifetime at the surface is lower than its bulk counterpart, the time constant τ_{eff} can be determined by τ_S during the initial period of the photoconductive decay. Due to the diffusion of the excess carriers from the near-surface region into the bulk region, the bulk recombination may dominate τ_{eff} at the later part of the PCD. As a result, the waveform consists of two slopes, with the larger one characterizing the surface recombination. This PCD behavior can be observed in the case of intense surface recombination, and the time constant of the measuring setup allows one to detect rapid signal decay. Taking this into account, it can be concluded that the PCD waveforms shown in Fig. 2 can be explained by the SRH recombination in the bulk.

The dark current in InSb photodiodes was analyzed previously in [7]. At low forward and reverse biases, it is determined by the generation and recombination processes in the depletion region. The forward current density is described by the expression $J = J_0 \exp(qU/\beta kT)$ with the ideality coefficient $\beta = = 1.7$. The reverse current-voltage characteristic is approximated by a power-law dependence $I \sim U^m$ with an exponent m equals 0.4–0.6 in the voltage interval $U = 10\text{–}200$ mV. This means that the carrier generation in the depletion region dominates the reverse current, which can be approximated as $J = = qn_iW/2\tau_0$, where W is the depletion region width, and τ_0 is the effective lifetime related to the steady-state lifetime of minority carriers [2]. According to the SRH model, the main contribution to the generation current is given by levels near the middle of the band gap. In this case, the effective generation time cannot be less than the sum $\tau_0 = \tau_{n0}+\tau_{p0}$ [11, 21]. Therefore, in the absence of a minority carrier trapping, the generation time in studied photodiodes should be close to $\sim 10^{-6}$ s. However, experimental values were found to range from $\sim 10^{-7}$ s to $\sim 10^{-9}$ s [7, 10]. In this regard, it is necessary to note the following feature of diffused photodiodes. The fact is that, in these photodiodes, depending on the fabrication conditions, a compensated region can be formed, resulting in the formation of a p^+-n^--n-type junction. This region mainly determines the width of the depletion region of the photodiodes. The electron density in the compensated region, determined from capacitance-voltage measurements, was found to be 3–5 times lower than in the starting material. This means that the minority carrier trapping in the compensated region can be more efficient than in the quasi-neutral region beyond, resulting in the trap-assisted tunneling current domination in the photodiodes [7]. In implanted photodiodes, the generation time of the order of 10^{-8} s was also reported in the literature [2]. In addition, since the studied photodiodes had a relatively large area of p-n junctions, on the order of 10^{-2}–10^{-3} cm^2, the contribution of the mesa surface to the dark current can be neglected.

Despite the fact that deep defects in InSb have been studied both experimentally and theoretically over a long period of time [7, 19, 22–24], in most published works, their parameters were determined by indirect methods, and the nature of the defects remained unclear. It was found that the density and

cross-section of deep defects are in the ranges of 10^{12}–10^{14} cm^{-3} and 10^{-12} to 10^{-17} cm^2, respectively. As for the defects with energy levels near the middle of the gap, they turned out to be independent of the growth method, doping, and type of conductivity. Most likely, these are structural defects. The theoretical progress in understanding the nature of point defects has been achieved with the use of the density functional theory [22–27]. The main point defects in InSb are vacancies, interstitial atoms, In_{Sb} and Sb_{In} antisites, and their complexes. The In_{Sb} and Sb_{In} antisites are acceptors and donors, respectively, which can exist in charge states $0/-1$ and $+1/0$. The formation energies of In_{Sb} and Sb_{In} antisites (1.46 and 1.29 eV, respectively) are significantly lower than those of In and Sb vacancies (2.57 and 1.69 eV, respectively). This means that antisites predominate over vacancies under stoichiometric conditions. Their ionization energies are close to $E_g/2$, namely, $E(0/-1) = 0.11$ eV and $E(+1/0) = 0.09$ eV. It can be assumed that the observed structural defects with states in the middle of the band gap are associated with antisites.

The conductivity type conversion in n-InSb subjected to the vacuum annealing could be explained by the formation of In_{Sb} antisites as a result of the preferential evaporation of the volatile component (Sb) [28]. Together with In vacancies and residual acceptors, they can determine the hole density in vacuum-annealed samples. However, the experimental confirmation of this phenomenon has not been obtained yet. To suppress the evaporation of Sb during the fabrication of diffused photodiodes, an additional amount of material was placed in a quartz ampoule [10]. Of course, the impurity diffusion and heat treatment can lead to the appearance of different defects. Thus, the minority carrier trapping in heat-treated samples and the trap-assisted tunnelling in photodiodes can also be associated with different traps. To some extent, this problem is similar to that observed in HgCdTe alloys [9]. So, the further research is needed to solve it.

The nature of $E3$ acceptor-like defects is not clear. A possible reason for their occurrence may be the retrograde solubility of cadmium in InSb. As a result, the point and extended defects may arise during the manufacture of p-n junctions in diffused photodiodes. In this regard, we note that, in the heat-treated samples, there was an increase in the density of etch pits associated with dislocations, as well as their nonuniform distribution. It is known that dislocations can create acceptor states in n-type A_3B_5 semiconductors, leading to a decrease in the electron density in the conduction band [29].

4. Conclusions

In this work, a model of two independent levels of acceptor-like traps and donor-like recombination centers is used to fit the experimental data in n-InSb. Within this model, the lifetime of excess carriers can be simulated over a wide range of temperatures without involving other recombination mechanisms. It is found that the level of acceptor-like traps is at a distance of about 70 meV below the edge of the conduction band. Their density is estimated to be of the order of 10^{13} cm^{-3}. It is most likely that traps are process-induced defects.

APPENDIX

1. A review of recombination mechanisms in narrow-gap semiconductors is carried out by Lopez *et al.* [1]. Using appropriate expressions, the lifetime of excess carriers was calculated. The main drawback of the theory developed by Beatty and Landsberg for the Auger-1 mechanism is the uncertainty in the value of the overlap integrals, which varies between 0.1 and 0.3, leading to an order of magnitude uncertainty in the carrier lifetime. As can be seen from Fig. 3, by varying the product of the overlap integrals, it is possible to fit the experimental and calculated data at high temperatures. To obtain agreement over the entire temperature range, it is necessary to allow an increase in the carrier density by an order of magnitude compared to the value in the reference samples, which cannot be justified.

2. With regard for the sufficiently small density of recombination and trapping centers, large difference between $E2$ and $E3$ levels, and asymmetry of the capture coefficients, the probability of intercenter transitions can be neglected. According to Wertheim [13], for a recombination mechanism involving two levels, the addition of reciprocal time constants is justified, if one of them is negatively charged. In this case, the net recombination rate can be represented by the sum of two individual rates [18]

$$R_n = -\frac{dn}{dt} = C_{n2}N_{t2}[n(1-f_{t2}) - n_{12}f_{t2}] + C_{n3}N_{t3}[n(1-f_{t3}) - n_{12}f_{t3}], \quad \text{(A1)}$$

$$R_p = -\frac{dp}{dt} = C_{p2}N_{t2}[pf_{t2} - p_{12}(1-f_{t2})] + C_{p3}N_{t3}[pf_{t3} - p_{12}(1-f_{t3})], \quad \text{(A2)}$$

where f_{t2} and f_{t3} denote the occupation probabilities for $E2$ and $E3$ levels. Since the level $E2$ lies deep in the band gap, the probability $f_{t2} \approx 1$. Neglecting the thermal emission from both levels to the bands, expression (10) for the minority lifetime can be obtained from (A1). The solution for the majority carrier lifetime is given by expression (11).

1. V.C. Lopes, A.J. Syllaios, M.C. Chen. Minority carrier lifetime in mercury cadmium telluride. *Semicond. Sci. Technol.* **8**, 824 (1993).
2. A. Rogalski. *Infrared Detectors*, 2nd edn. (Boca Raton, CRC Press, Taylor & Francis Group, 2011).
3. R.A. Laff, H.Y. Fan. Carrier lifetime in indium antimonide. *Phys. Rev.* **121**, 53 (1961).
4. J.E.L. Hollis, C. Choo, E.L. Heasell. Recombination centers in InSb. *J.Appl. Phys.* **35**, 1626 (1967).
5. Y. Tokumaru, H. Okushi, H. Fujisada. Deep levels in n-type undoped and Te-d oped InSb crystals. *Jap. J. Appl. Phys.* **26**, 499 (1987).
6. K. Tsukioka, H. Miyazawa. DLTS studies on InSb p-n^+ diodes. *Jap. J. Appl. Phys.* **21**, L526 (1982).
7. V.V. Tetyorkin, A.V. Sukach, A.I. Tkachuk. Infrared photodiodes on II–VI and III–V narrow gap semiconductors. In: *Photodiodes – from Fundamentals to Applications.* Edited by Prof. Ilgu Yun (InTechopen, 2012).
8. R. Fastow, D. Goren, Y. Nemirovsky. Shockley-read recombination and trapping in p-type HgCdTe. *Appl. Phys. Lett.* **68**, 3405 (1990).
9. Y. Nemirovsky, R. Fastov, A. Adar, A. Unikovsky. Trapping effects in HgCdTe. *J. Vac. Sci. Technol. B* **9**, 1829 (1991).
10. A.V. Sukach, V.V. Tetyorkin, A.I. Tkachuk. Electrical properties of InSb p-n junctions prepared by diffusion method. *SPQE* **19**, 295 (2016).
11. W. Shockley, W.T. Read Jr. Statistics of the recombination of holes and electrons. *Phys. Rev.* **87**, 835 (1952).
12. D.J. Sandifford. Carrier lifetime in semiconductors for transient conditions. *Phys. Rev.* **105**, 524 (1957).
13. G.K. Wertheim. Transient recombination of excess carriers in semiconductors. *Phys. Rev.* **109**, 1086 (1958).
14. J.S. Blakmore. *Semiconductor Statistics* (Pergamon Press, 1962).
15. J. Reichman. Minority carrier lifetime of HgCdTe from photoconductivity decay method. *Appl. Phys. Lett.* **59**, 1221 (1991).
16. K. Heyke, G. Lautz , H. Schumny. Current noise in n-type InSb. *Phys. Stat. Sol. (a)* 1970. **1**, (1970).
17. M.A. Sipovskaya, Yu.S. Smetannikova. Dependence of the lifetime of current carriers in n-InSb on the electron density. *Sov. Phys. Semicond.* **18**, 356 (1984) (In Russia).
18. A. Schenk, U. Krumbein. Coupled defect-level recombination: theory and application to anomalous diode characteristics. *J. Appl. Phys.* **78**, 3185 (1995).
19. D.K. Schroder. *Semiconductor Material and Device Characterization* (Wiley, 2006) [ISBN: 978-0-471-73906-7].
20. P.J. Drummond, D. Bhatia, A. Kshirsagar, S. Ramani, J. Ruzyllo. Studies of photoconductance decay method for characterization of near-surface electrical properties of semiconductors. *Thin Solid Films* **519,** 7621 (2011).
21. S.M. Sze, Kwok K. Ng. *Physics of Semiconductor Devices, 3d. ed.* (Wiley, 2007).
22. O. Madelung. *Semiconductors – Basic Data* (Springer, 1996).
23. O. Madelung, U. Rössler, M. Schulz. *Landolt-Börnstein – Group III Condensed Matter. Numerical Data and Functional Relationships in Science and Technology. Vol. 41A2b. Impurities and Defects in Group IV Elements, IV–IV and III–V Compounds. Part b: Group IV–IV and III–V Compounds* (Springer, 2003).
24. C. Littler. Characterization of impurities and defects in InSb and HgCdTe using novel magneto-optical techniques. *Proc. SPIE* **2021**, 184 (1993).
25. A. Chroneos, H.A. Tahini, U. Schwingenschlögl, R.W. Grimes. Antisites in III–V semiconductors: Density functional theory calculations. *J. Appl. Phys.* **116**, 023505 (2014).
26. H.A. Tahini, A. Chroneos, S.T. Murphy, U. Schwingenschlögl, R.W. Grimes. Vacancies and defect levels in III–V semiconductors. *J. Appl. Phys.* **114**, 063517 (2013).
27. A. Höglund, C.W.M. Castleton, M. Göthelid, B. Johansson, S. Mirbt. Point defects on the (110) surfaces of InP, InAs, and InSb: A comparison with bulk. *Phys. Rev. B* **74**, 075332 (2006).
28. S.V. Stariy, A.V. Sukach, V.V. Tetyorkin, V.O. Yukhymchuk, T.R. Stara. Effect of thermal annealing on electrical and photoelectrical properties of n-InSb. *SPQEO* **20**, 105 (2017).
29. J.H. You, H.T. Johnson. Effect of dislocations on electrical and optical properties in GaAs and GaN. *Solid State Phys.* **61**, 143 (2009).

Received 19.10.23

В.В. Тетьоркін, А.І. Ткачук, І.Г. Луцишин

РЕКОМБІНАЦІЯ ТА ПРИЛИПАННЯ НЕРІВНОВАЖНИХ НОСІЇВ В n-InSb

В статті досліджується вплив ефекту прилипання на перехідний і стаціонарний час життя нерівноважних носіїв заряду для зразків InSb провідності n-типу. Вимірювання кінетики фотопровідності та постійного струму було використано для характеристики вихідного матеріалу та інфрачервоних фотодіодів. Велика різниця між перехідним і стаціонарним часом життя пояснюється прилипанням неосновних носіїв на акцепторних пастках у рамках моделі дворівневої рекомбінації. Оцінено рекомбінаційні параметри пасток.

Ключові слова: InSb, нерівноважні носії, час життя, рекомбінація, прилипання, інфрачервоні фотодіоди.